Int. J. Solids Structures Vol. 17, pp. 451–470, 1981
Printed in Great Britain.

0020-7683/81/050451-20$02.00/0
Pergamon Press Ltd.

SHEAR BAND FORMATION IN PLANE STRAIN

J. W. HUTCHINSON
Division of Applied Sciences, Harvard University, Cambridge, MA 02138, U.S.A.

and

V. TVERGAARD
Department of Solid Mechanics, Technical University of Denmark, Lyngby, Denmark

(*Received* 22 *June* 1980; *in revised form* 22 *September* 1980)

Abstract—The growth of a single shear band in an infinite block of an incompressible solid undergoing plane strain tension or compression is studied for three material models—nonlinear elasticity, kinematic hardening plasticity and a plasticity theory based on yield surface corner development. The study includes analyses of bifurcation and post-bifurcation behaviour as well as the sensitivity of shear band growth to material imperfections. Depending on their orientation and on details of the material model, shear bands may form gradually with relatively limited localization of strain or they may localize catastrophically with an attendant strong sensitivity to initial imperfections in the form of material inhomogeneity.

1. INTRODUCTION

For ductile metals localization of plastic flow into one or several shear bands is often observed when the fundamental smoothly varying deformations have reached a certain critical level. The conditions for bifurcation into a shear band have been given by Hill[1], by Rudnicki and Rice[2] and by Rice[3], who also gives a discussion of several aspects of shear band localization for various material models. For the classical elastic–plastic solid with a smooth yield surface no bifurcation into a shear band is predicted at a realistic level of straining, unless the strain hardening level is very low. However, the critical strain is considerably lowered by the assumption that a vertex develops at the current stress point on subsequent yield surfaces. Another deviation from the assumptions of classical plasticity theory that significantly reduces the critical strain for shear band formaion is the plastic dilation that will appear as the macroscopic effect of the nucleation and growth of microscopic voids in a ductile material, as has been discussed by Yamamoto[4] and Needleman and Rice[5].

In the present paper shear band formation in an incompressible material is considered under conditions of plane strain, for which bifurcation has been analysed in detail by Hill and Hutchinson[6]. The development of shear bands beyond bifurcation is analysed both asymptotically and numerically on the basis of three different constitutive descriptions. The study emphasizes the character of the growth process as dependent on the material model. One of the models considered is a phenomenological corner theory of plasticity recently developed by Christoffersen and Hutchinson[7]; the second is the purely elastic material (a large strain generalization of J_2 deformation theory) that is also chosen to represent the response in the total loading region of the vertex model; and the third is a flow theory of plasticity with kinematic hardening.

The critical bifurcation strain for the purely elastic solid is identical to that of the vertex model. However, the post-bifurcation behaviour and the imperfection-sensitivity found for the two materials differ considerably. In fact, even for the corner theory the behaviour after bifurcation is sensitive to details of the vertex description. In some cases it is found that the vertex model predicts early saturation of shear bands orientated such that they set in at the lowest strain levels, whereas bands developing at later stages experience continued localized shearing. This behaviour agrees qualitatively with experimental observations of shear band formation in a high strength maraging steel made by Anand and Spitzig[8].

The results for a kinematically hardening solid are included here to show that shear band localization at a realistic strain level may be predicted even for a smooth yield surface, provided that there is a small initial material inhomogeneity. The predictions for the kinematically hardening solid are not unlike those for the solid which develops a corner, although for

very small initial inhomogeneities the bands occur only at large strains in the kinematically hardening solid.

In all cases in this paper, only the simplest of shear bands is analysed where the band is assumed to be of constant width and infinite extent so that there is no variation in behaviour along the band. The more difficult problem involving growth of a band of finite extent from some initial inhomogeneity or geometric imperfection has only just recently been attempted by Tvergaard *et al.*[9] for a plane strain tension specimen and by Knowles and Sternberg[10] and Abeyaratne[11] for bands emanating from the tip of a crack in anti-plane shear.

2. SHEAR BAND BIFURCATIONS

Conditions for shear band bifurcations in time-independent solids have been given by Hill[1], Rudnicki and Rice[2] and Rice[3]. Here we quickly restate the bifurcation results of Hill and Hutchinson[6] for the onset of shear bands in an incompressible, time-independent solid subject to plane strain tension or compression.

An infinite block of material is assumed to be incompressible, homogeneous and orthotropic with respect to the x_i axes in the current state. The Cartesian components of the Cauchy stress in the (x_1, x_2) plane are

$$\sigma_{11} = \sigma, \qquad \sigma_{22} = 0, \qquad \sigma_{12} = 0. \tag{2.1}$$

If the material is incrementally linear, an incremental plane strain response is governed by two positive instantaneous shearing moduli μ and μ^* where

$$\overset{*}{\sigma}_{11} - \overset{*}{\sigma}_{22} = 2\mu^*(\dot{\epsilon}_{11} - \dot{\epsilon}_{22}), \qquad \overset{*}{\sigma}_{12} = 2\mu\dot{\epsilon}_{12}, \qquad \dot{\epsilon}_{11} + \dot{\epsilon}_{22} = 0. \tag{2.2}$$

Here $\overset{*}{\sigma}_{ij}$ are the Cartesian components of the Jaumann co-rotational rate of the Cauchy stress and $\dot{\epsilon}_{ij}$ is the Eulerian strain-rate. Shearing at 45° to the (x_1, x_2) axes is governed by μ^*; $4\mu^*$ is also the tangent modulus for a plane strain increment of stressing parallel to the x_1 axis. The fundamental, or uniform, solution increment satisfies

with

$$\left.\begin{aligned} &\dot{\sigma} = 4\mu^*\dot{\epsilon} \\ &\overset{*}{\sigma}_{11} = \dot{\sigma}, \qquad \overset{*}{\sigma}_{12} = \overset{*}{\sigma}_{22} = 0 \\ &\dot{\epsilon}_{11} = -\dot{\epsilon}_{22} = v_{1,1} = -v_{2,2} = \dot{\epsilon}, \qquad \dot{\epsilon}_{12} = v_{1,2} = v_{2,1} = 0 \end{aligned}\right\} \tag{2.3}$$

where $v_i(x_1, x_2)$, $i = 1, 2$ are the velocity components.

As shown in Fig. 1, ψ is the angle between the incipient shear band normal ν and the x_1-axis while t is the shearing direction so that

$$(\nu_1, \nu_2) = (\cos\psi, \sin\psi), \qquad (t_1, t_2) = (-\sin\psi, \cos\psi). \tag{2.4}$$

Here we restrict attention to shear band solutions with uniform strains and rotations in an infinite band of constant width. The eigenmodal velocity gradients in the band associated with bifurcation into such a solution are

$$v_{i,j} = \dot{a} t_i \nu_j. \tag{2.5}$$

The complete bifurcation mode is a linear combination of the fundamental increment (2.3), and (2.5) where the amplitude factor $\dot{a}$ is determined by post-bifurcation considerations.

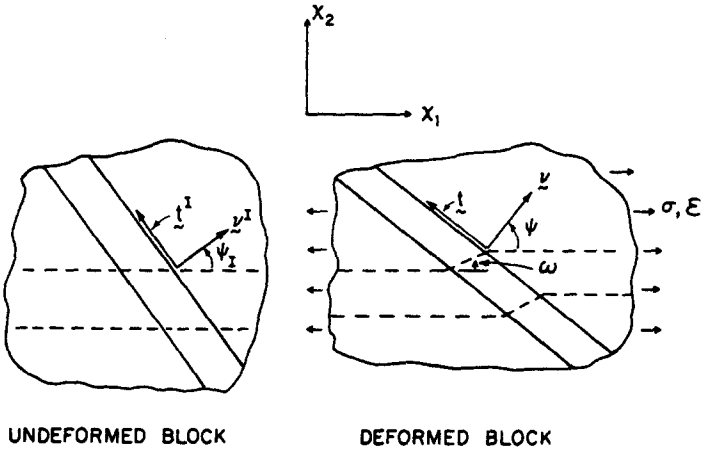

Fig. 1. Shear band in an infinite block of material.

The bifurcation condition for the onset of a shear band with orientation ψ is [6]

$$\left(\mu - \frac{1}{2}\sigma\right)\tan^4\psi + 2(2\mu^* - \mu)\tan^2\psi + \left(\mu + \frac{1}{2}\sigma\right) = 0. \tag{2.6}$$

If

$$\mu > |\sigma/2| \quad \text{and} \quad 2\mu^* > \mu - (\mu^2 - \sigma^2/4)^{1/2} \tag{2.7}$$

there are no real solutions for $\tan\psi$ to (2.6); the equations governing an incremental response of the block are elliptic and shear bands are not possible. However, if

$$\mu > |\sigma/2| \quad \text{and} \quad 2\mu^* < \mu - (\mu^2 - \sigma^2/4)^{1/2} \tag{2.8}$$

the equations are hyperbolic and there are two solutions for $\tan^2\psi$. If $\mu < |\sigma/2|$ there is only one solution. This is the parabolic case; it will not be encountered in this paper. Assuming (2.8) holds, one can arrange the solutions for $\tan^2\psi$ into the form

$$\tan^2\psi = 1 + \frac{\sigma - 4\mu^* \pm [(\sigma - 4\mu^*)^2 - 8\mu^*(2\mu - \sigma)]^{1/2}}{2\mu - \sigma} \tag{2.9}$$

where the reality of the square root is ensured by (2.8).

Conditions (2.8) imply $\sigma^2 > 16\mu^*(\mu - \mu^*)$ and $\mu > 2\mu^*$ from which it follows that $\sigma^2 > 16\mu^{*2}$. Thus it can be seen immediately from (2.9) that for plane strain tension ($\sigma > 0$) both orientations satisfy

$$\tan^2\psi > 1 \quad \text{or} \quad |\psi| > \pi/4. \tag{2.10}$$

As noted by Nemat-Nasser *et al.* [12], the angle between the shear band normal and tensile axis is always greater than 45° at bifurcation in plane strain tension.

Given any shear band solution in the incompressible block under plane strain tension ($\sigma_{11} = \sigma$), the corresponding solution under plane strain compression ($\sigma_{22} = -\sigma$) is obtained by superposition of a hydrostatic pressure $\sigma_{ij} = -\sigma\delta_{ij}$. Thus if ψ gives the current orientation of the band in plane strain tension, then the normal to the band in the corresponding plane strain compression solution makes an angle $\pi/2 - \psi$ to the x_2 compression axis. From (2.10), the angle between the band normal and the compression axis at bifurcation is always less than 45°. If ϵ is the logarithmic strain in the x_1 direction in the tension problem, then $-\epsilon$ is the compressive strain in the x_2 direction in the corresponding compression problem. All results presented below

will be for plane strain tension, but they can be converted to the compression case with the aid of the above observations.

In a history of monotonic straining from the unstressed state the inequalities associated with ellipticity (2.7) will generally hold at low strains. For the constitutive laws considered in this paper, ellipticity is first lost with the possible emergence of shear bands when the equality in the second of the conditions (2.7) is met, i.e. when

$$\sigma_c^2 = 16\mu^*(\mu - \mu^*) \quad \text{with} \quad \mu > |\sigma_c/2|. \tag{2.11}$$

This will be referred to as the *critical bifurcation stress.* The associated *critical shear band orientation* from (2.9) is

$$\tan^2 \psi_c = 1 + \frac{\sigma_c - 4\mu^*}{2\mu - \sigma_c} = \left(\frac{2\mu + \sigma_c}{2\mu - \sigma_c}\right)^{1/2}. \tag{2.12}$$

3. BIFURCATION AND POST-BIFURCATION BEHAVIOUR OF A SHEAR BAND IN A NONLINEAR ELASTIC SOLID IN PLANE STRAIN

In plane strain, an isotropic, incompressible nonlinear elastic solid has a strain energy density W which is a function of the maximum principal stretch λ, or equivalently the maximum principal logarithmic strain $\epsilon = \ln \lambda$. With the (x_1, x_2) axes coincident with the principal axes and with $\epsilon_1 = -\epsilon_2 = \epsilon$ [13],

$$\left.\begin{aligned} \sigma_1 - \sigma_2 &= \lambda \, \mathrm{d}W/\mathrm{d}\lambda = \mathrm{d}W/\mathrm{d}\epsilon \\ 2\mu &= \frac{\lambda^4 + 1}{\lambda^4 - 1}(\sigma_1 - \sigma_2) = \coth(2\epsilon)(\sigma_1 - \sigma_2) \\ 4\mu^* &= \lambda \frac{\mathrm{d}}{\mathrm{d}\lambda}(\sigma_1 - \sigma_2) = \frac{\mathrm{d}^2 W}{\mathrm{d}\epsilon^2}. \end{aligned}\right\} \tag{3.1}$$

We will illustrate the development of a shear band for a specific power-law material which in plane strain is specified in terms of the maximum principal logarithmic strain by

$$W = \frac{k}{N+1}\epsilon^{N+1} \tag{3.2}$$

where N is a "hardening" exponent which falls in the range $0 < N \leq 1$. In plane strain tension ($\sigma_1 = \sigma$, $\sigma_2 = 0$) this gives

$$\sigma = k\epsilon^N \tag{3.3}$$

and

$$4\mu = kq\epsilon^{N-1}, \qquad 4\mu^* = kN\epsilon^{N-1} \tag{3.4}$$

where

$$q(\epsilon) = 2\epsilon \coth(2\epsilon). \tag{3.5}$$

Bifurcation

For the power-law material it is readily shown that the critical bifurcation strain associated with shear band bifurcation from (2.11) satisfies

$$\epsilon_c = [N(q(\epsilon_c) - N)]^{1/2} \tag{3.6}$$

and the associated critical shear band orientation (2.12) is given by

$$\tan \psi_c = e^{\epsilon_c} = \lambda_c. \tag{3.7}$$

(The opposite-signed orientation is also possible; but, for simplicity of presentation, we will always consider only positive orientations ψ with the sense shown in Fig. 1.)

If ψ_I is the orientation of a material line (e.g. a potential band as in Fig. 1) in the undeformed state, its orientation ψ following a uniform strain ϵ in the x_1-direction is given by

$$\tan \psi = e^{2\epsilon} \tan \psi_I. \tag{3.8}$$

A simple property of the critical bifurcation solution for the power-law material which follows directly from (3.7) and (3.8) is

$$\psi_c + \psi_I = \pi/2 \tag{3.9}$$

where ψ_I is the orientation of the band material in the undeformed state.

Figure 2 displays the critical strain and the associated band orientation ψ_c as a function of N as determined from (3.6) and (3.7). For small N, $\epsilon_c \cong \sqrt{N}$ and $\psi_c \cong 45°$. In the next subsection a numerical analysis of the finite amplitude response following bifurcation is given, including the influence of initial material inhomogeneity. Following that, analytical results are given for the initial post-bifurcation behaviour and imperfection-sensitivity.

Post-bifurcation and imperfection-sensitivity: numerical results

Attention is restricted to shear bands which are straight with infinite extent as depicted in Fig. 1. The displacement gradients and stresses are uniform inside and outside the band with discontinuities in certain components across the boundaries of the band, consistent with continuity of traction and displacement. The width of the band does not arise as a variable in the analysis when the band is infinite. The state outside the band is required to be one of plane strain tension aligned with the x_1-direction. Finite discontinuities of this type have been studied in some detail by Knowles and Sternberg[14], who call them strong shocks in analogy to discontinuities in fluid mechanics.

When the material is homogeneous in the underformed state the body will be said to be perfect. We will also consider an imperfect body in which an initial inhomogeneity is specified in the form of a band of material with uniform properties which are slightly different from those of the exterior regions. The orientation of this band in the undeformed state, ψ_I, can be specified arbitrarily. The numerical examples presented below are based on the power-law material (3.2). We take $k = k_0$ outside the band and $k = k_b$ inside the band and introduce a

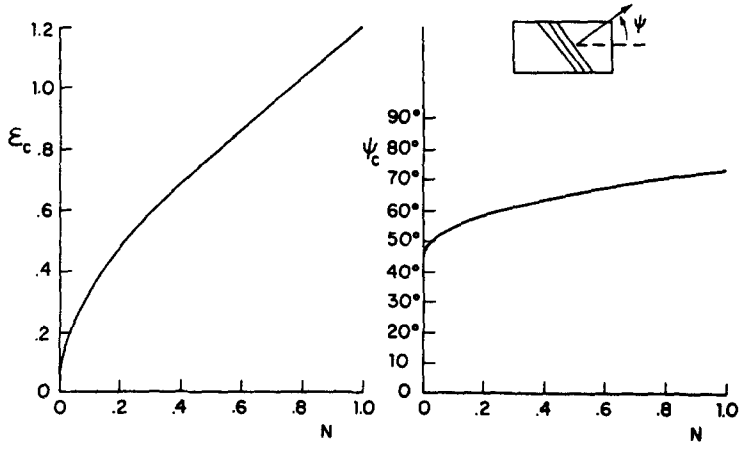

Fig. 2. Critical strain ϵ_c and associated band orientation ψ_c as functions of the strain hardening exponent N.

measure of the imperfection as

$$\bar{\xi} = (k_0 - k_b)/k_0 \tag{3.10}$$

so that $\bar{\xi} > 0$ implies that the band material is softer than the outside material.

With x_i $(i = 1, 2)$ as Cartesian axes, let $u_i(x_j)$ denote the displacement components referred to these axes of a material point initially at x_j. Let σ_{ij} denote the Cauchy stress components referred to the x_i-axes. Quantities inside the band will be labelled by a superscript or subscript b while outside the band the label will be 0. Outside the band a state of plane strain tension is prescribed such that the x_i-axes are principal with stretches $\lambda_1{}^0 = 1/\lambda_2{}^0 \equiv \lambda$ and with

$$u^0_{1,1} = (\lambda - 1), \qquad u^0_{2,2} = (\lambda^{-1} - 1), \qquad u^0_{1,2} = u^0_{2,1} = 0 \tag{3.11}$$

$$\sigma^0_{11} \equiv \sigma, \qquad \sigma^0_{22} = \sigma^0_{12} = 0. \tag{3.12}$$

The logarithmic strain $\epsilon = \ln \lambda$ outside the band will be regarded as the independent variable specifying the applied deformation. The stresses and strains are taken to be related through $(3.1)_1$.

Inside the band the four displacement gradients $u^b_{i,j}$ are constrained by the condition of incompressibility which can be stated as

$$u^b_{1,1} + u^b_{2,2} + u^b_{1,1}u^b_{2,2} - u^b_{1,2}u^b_{2,1} = 0. \tag{3.13}$$

Continuity of displacements across the interfaces between the band and the exterior regions requires

$$(u^b_{i,j} - u^0_{i,j})t^I_j = 0 \tag{3.14}$$

where $\mathbf{t}^I = (-\sin\psi_I, \cos\psi_I)$ is the tangent vector to the band material in the undeformed state. The Lagrangian strain tensor in the band is

$$\eta^b_{ij} = \frac{1}{2}(u^b_{i,j} + u^b_{j,i}) + \frac{1}{2}u^b_{k,i}u^b_{k,j}. \tag{3.15}$$

With x'_i denoting the principal axes of $\boldsymbol{\eta}^b$ and with $\eta_{1'}{}^b$ and $\eta_{2'}{}^b$ as the principal components, the principal logarithmic strains in the band are

$$\epsilon_{1'}{}^b = -\epsilon_{2'}{}^b = \frac{1}{2}\ln(1 + 2\eta_{1'}{}^b). \tag{3.16}$$

From $(3.1)_1$

$$\sigma_{1'}{}^b - \sigma_{2'}{}^b = \mathrm{d}W/\mathrm{d}\epsilon_{1'}{}^b. \tag{3.17}$$

Continuity of traction across the band interfaces requires

$$(\sigma^b_{ij} - \sigma^0_{ij})\nu_i\nu_j = 0 \tag{3.18}$$

and

$$(\sigma_{ij}{}^b - \sigma_{ij}{}^0)\nu_i t_j = 0 \tag{3.19}$$

where $\boldsymbol{\nu}$ and $\mathbf{t}$ are the current unit normal and tangent vectors to the band defined in (2.4).

The simple numerical scheme used to calculate the shear band solutions was formulated as follows. Of the four displacement gradients in the band, $x \equiv u^b_{1,2}$ and $y \equiv u^b_{2,1}$ are chosen as unknown variables, while $u^b_{1,1}$ and $u^b_{2,2}$ are expressed directly as linear combinations of x and y

with the aid of the two displacement continuity equations (3.14). The incompressibility constraint (3.13) provides one equation for x and y. The second is (3.19) which reduces to

$$(\sigma_{1'}{}^{b} - \sigma_{2'}{}^{b}) \sin 2(\psi - \alpha) - \sigma \sin 2\psi = 0 \tag{3.20}$$

where α is the angle between the principal x_1'-axis in the band and the x_1-axis. The unknowns x and y enter into (3.20) in a highly nonlinear way through (3.13) and through rotation to the principal strain axes where (3.16) and (3.17) are used. This, however, presents no difficulty in the numerical procedure. The two equations in x and y are solved using a standard Newton–Raphson method in which derivatives with respect to x and y needed in each iteration are evaluated numerically. The remaining eqn (3.18) is not needed in the determination of x and y but can be used to determine the jumps in the hydrostatic stress component across the band interface once x and y are known.

The numerical results shown in Fig. 3 are for the power-law material (3.2) with $N = 0.1$ and these are typical for other N-values. The growth of the shear band as measured by the angle ω is shown as a function of the strain ϵ outside the band. The angle ω (see Fig. 1) is that made with the x_1-axis by a material line element in the band which is initially parallel to the x_1-axis; ω is given by

$$\sin \omega = u^b_{2,1}[(1 + u^b_{1,1})^2 + u^b_{2,1}]^{-1/2}. \tag{3.21}$$

The critical bifurcation for the perfect block is $\epsilon_c = 0.32$ when $N = 0.1$ with $\psi_c = 54.2°$. In all cases shown in Fig. 3, perfect and imperfect, the initial band orientation is taken as $\psi_I = \pi/2 - \psi_c = 35.8°$, which, from (3.9), corresponds to the initial orientation associated with the critical bifurcation. The subsequent orientation of the band is given by (3.8). The relation between ω and ϵ is independent of k_0 in the perfect case, while in the imperfect case it depends on $\bar{\xi}$ defined in (3.10) but not otherwise on k_0 and k_b.

When the material in the band is softer than that outside the band ($\bar{\xi} > 0$) the response leads to negative ω with shearing in the direction one would expect. The response is highly imperfection-sensitive in the sense that a very small softening in the band results in a substantial reduction in the maximum strain ϵ_{max} which can be achieved outisde the band. A

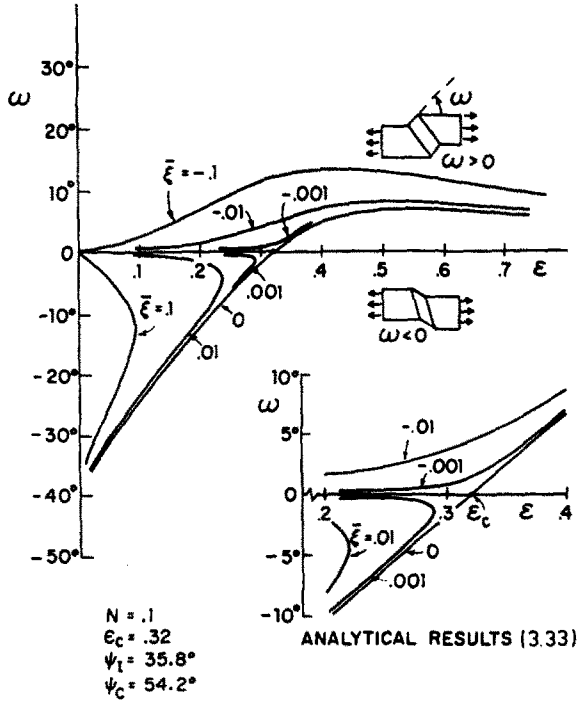

Fig. 3. Post-bifurcation behaviour and imperfection-sensitivity in a nonlinear elastic solid.

one percent difference between k_b and k_0 results in a thirty percent reduction in ϵ_{max}. More will be said of this below. When $\bar{\xi} < 0$, the material in the band is harder than that outside and the opposite-signed shearing takes place. While these responses are actual solutions, they are artificial in that the shear deformation is only permitted within the band. Bifurcation outside the band would certainly occur for $\epsilon > \epsilon_c$ if permitted.

Initial post-bifurcation and imperfection-sensitivity-analytical results

The behaviour of the solutions in the vicinity of the bifurcation point is amenable to a perturbation analysis in the spirit of Koiter's[15] approach to initial post-buckling behaviour and imperfection-sensitivity. Koiter's approach was not intended for problems in which ellipticity is lost, but the formalism carries over to the nonlinear algebraic equations governing the present problem. Budiansky's[16] version of Koiter's theory is based on a singular perturbation expansion of the equilibrium equations, rather than of the energy functional used by Koiter and Budiansky's version appeared to be the more convenient for arriving at the expansions given below. The conversion from Budiansky's formalism to the results given below is relatively straightforward, and thus we will omit details and give only the end results.

As in the previous subsection, the current band orientation at strain $\epsilon = \ln \lambda$ outside the band is specified by ψ in (3.8) where ψ_I is the initial orientation. The material outside the band is isotropic and incompressible and is specified by $W(\lambda_1)$ as in (3.1), where λ_1 is the maximum principal stretch. Inside the band the strain energy density is taken to be

$$(1 - \bar{\xi}) W(\lambda_1) \tag{3.22}$$

so that $\bar{\xi} > 0$ corresponds to a softer material inside the band than outside. With $\bar{\xi} = 0$ the material is initially homogeneous.

Denote the displacement gradients in the fundamental solution of the perfect case ($\bar{\xi} = 0$) given in (3.11) by $u^0_{i,j}(\lambda)$. Outside the band the fundamental solution is always in force and the stretch there, λ, is again regarded as the applied deformation parameter. For the perfect case bifurcation occurs at λ_c and the eigenmodal gradients in the band are

$$\xi u^{(1)}_{i,j} = \xi t^c_i \nu^I_j \tag{3.23}$$

where $\mathbf{t}^c$ is defined by (2.4) with $\psi = \psi_c$ and $\boldsymbol{\nu}^I$, the normal in the undeformed slab, is given by $(2.4)_1$ with $\psi = \psi_I$.† The expansion for the displacement gradients in the band has the form

$$u_{i,j} = u^0_{i,j}(\lambda) + \xi u^{(1)}_{i,j} + \xi^2 u^{(2)}_{i,j} + \cdots \tag{3.24}$$

where ξ is the amplitude of the eigenmodal contribution which plays the role of the expansion parameter.

With $\bar{\xi} = 0$, the initial post-bifurcation expansion relating λ and ξ is[15, 16]

$$\lambda = \lambda_c + A\xi + B\xi^2 + \cdots \tag{3.25}$$

while from (3.21)

$$\omega = \xi \lambda_c^{-1} \cos \psi_c \cos \psi_I + 0(\xi^2). \tag{3.26}$$

The bifurcation point is an asymmetric one and the exact result for A is given by

$$(\lambda_c + \lambda_c^{-1}) \frac{A}{\lambda_c} = \frac{3[(\lambda_c^2 + 1)^2 - 2(\lambda_c^4 + 1)P^2]P + \chi P^3}{2[-(\lambda_c^2 + 1)^2(1 + 2P^2) + 6(\lambda_c^4 + 1)P^2] - 2\chi P^2} \tag{3.27}$$

†To avoid introducing new notation in eqns (3.23)–(3.30), we now use a subscript or superscript c to denote quantities evaluated at the bifurcation point, whether or not bifurcation occurs at the critical (lowest) bifurcation point.

where

$$P = -\sin(\psi_I + \psi_c)$$

and

$$\chi = (\lambda_c^4 - 1)\left[\frac{\sigma - d\mu^*/d\epsilon}{\mu - \mu^*}\right]_{\lambda=\lambda_c}.$$

With $0 < |\bar{\xi}| \ll 1$, the asymptotic relation between λ, ξ and $\bar{\xi}$ in the vicinity of λ_c is [15, 16]

$$\lambda = \lambda_c + A\xi + \bar{\xi}\rho\lambda_c/\xi + \cdots \tag{3.28}$$

where the exact result for ρ is given by

$$\rho\lambda_c = \frac{(\lambda_c^2+1)(\lambda_c^4-1)P\sigma_c(\mu_c - \mu_c^*)^{-1}}{4[-(\lambda_c^2+1)^2(1+2P^2)+6(\lambda_c^4+1)P^2]-4\chi P^2}. \tag{3.29}$$

For $\bar{\xi}A\rho > 0$ there is a limit point in the relation of λ to ξ and from (3.28) the maximum λ is

$$\lambda_{max} = \lambda_c - 2(\bar{\xi}A\rho\lambda_c)^{1/2} + \ldots. \tag{3.30}$$

The strong imperfection-sensitivity of λ_{max} as implied by the square root dependence on the imperfection amplitude $\bar{\xi}$ is characteristic for elastic systems with an asymmetric bifurcation point.

We specialize the above results further to the power-law material (3.2). Furthermore, as in the example in Fig. 3, we choose ψ_I as the initial orientation associated with the *critical* bifurcation strain (3.6) so that relations (3.4)–(3.5), (3.7) and (3.9) hold, as do the curves in Fig. 2. In this case (3.27) and (3.29) become

$$A/\lambda_c = \frac{1}{2}(\lambda_c + \lambda_c^{-1})^{-1} \tag{3.31}$$

and

$$\rho = \frac{N(\lambda_c + \lambda_c^{-1})^2\epsilon_c^2}{(\lambda_c + \lambda_c^{-1})[4N\epsilon_c^2 + N^2(1-N)] - 3(\lambda_c - \lambda_c^{-1})\epsilon_c^3}. \tag{3.32}$$

These quantities are plotted in Fig. 4. With the aid of (3.26) and $\epsilon = \ln\lambda$, (3.28) may be

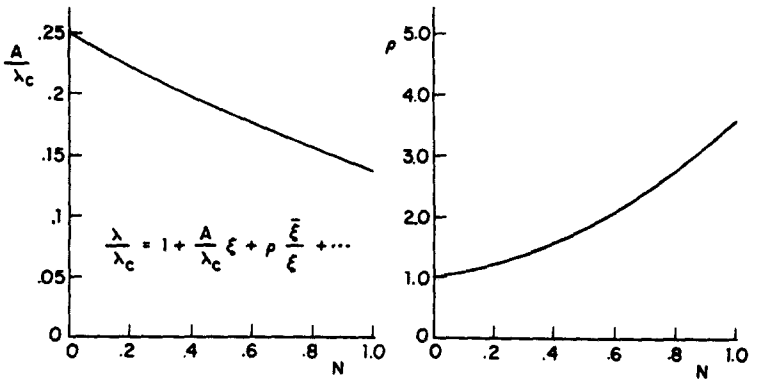

Fig. 4. Post-bifurcation parameters A and ρ for a nonlinear elastic solid as functions of the strain hardening exponent N.

re-expressed in terms of ϵ and ω as

$$\epsilon = \epsilon_c + \frac{A}{\cos\psi_0 \cos\psi_I}\omega + \bar{\xi}\rho\frac{\cos\psi_c \cos\psi_I}{\lambda_c \omega} + \ldots. \tag{3.33}$$

Curves of ω as function of ϵ from the asymptotic result (3.33) with $N = 0.1$ are shown as an insert in Fig. 3 where they can be compared with the unapproximated numerical results.

A revealing further simplification is found for small N (i.e. $0 < N \ll 1$). Then

$$\epsilon_c \cong \sqrt{N}, \qquad \psi_I \cong \psi_c \cong \pi/4, \qquad A \cong 1/4, \qquad \rho \cong 1$$

and (3.33) becomes

$$\epsilon \cong \epsilon_c + \frac{1}{2}\omega + \frac{1}{2}\bar{\xi}/\omega + \ldots. \tag{3.34}$$

For $\bar{\xi} > 0$,

$$\epsilon_{\max} \cong \epsilon_c - \sqrt{\bar{\xi}} + \ldots. \tag{3.35}$$

4. BIFURCATION AND POST-BIFURCATION BEHAVIOUR OF A SHEAR BAND IN PLASTIC SOLIDS

The bifurcation equations of Section 2 apply to a time-independent plastic solid under plane strain tension when the solid is taken to be incompressible and initially isotropic and when μ and $4\mu^*$ are identified with the instantaneous shearing modulus and plane strain tension modulus associated with the least stiff plastic loading branch currently available. For an elastic–plastic solid with a smooth yield surface μ is necessarily the instantaneous elastic modulus because the yield surface prevents a plastic shearing increment, $\dot{\epsilon}^p_{12}$, at bifurcation. Since $4\mu^*$ is the tangent modulus associated with plastic loading, it will generally be true that $4\mu^* \ll \mu$ well into the plastic range and from (2.11) the critical stress for the onset of a shear band is

$$\sigma_c \cong 2\sqrt{(4\mu^*\mu)}. \tag{4.1}$$

When μ is the elastic shear modulus, the bifurcation stress (4.1) is not likely to be attained even at very large strains in most structural metals deformed at room temperature, except at extremely low strain hardening (e.g. $\mu^*/\mu < 10^{-4}$).

If shear band formation is highly imperfection-sensitive in such a material it is possible that a small imperfection, such as slightly softer material in the band, will lead to pronounced shear band growth at moderately large strains even though (4.1) is not attained. This is, in fact, the situation for a solid characterized by kinematic hardening in which a smooth yield surface translates but does not expand, as will be seen below. When isotropic hardening is assumed even the imperfect block of material does not permit significant shear band growth, except possibly at very large strains.

If a corner, or vertex, develops at the loading point of the yield surface the instantaneous shearing modulus μ in a state of plane strain tension takes on a value which can be well below the elastic shear modulus. The critical bifurcation stress will therefore also be well below the corresponding critical stress for a solid with a smooth yield surface. Following the presentation of results for the kinematic hardening solid, we will discuss shear band development in perfect and imperfect blocks of a solid which permits corner formation. First, however, we give the incremental equations for an isolated shear band in a general incompressible solid undergoing plane strain tension or compression. The analysis is similar to that of Rice [3], although he does not restrict consideration to an incompressible solid.

The current orientation of the band is again specified by ψ as in Fig. 1. Outside the band plane strain tension is in force according to (3.11) and (3.12). With $v_i(x_1, x_2)$ as the velocity

components of a particle currently at (x_1, x_2) with respect to the Cartesian axes x_i,

$$\dot{\epsilon}_{ij} = \frac{1}{2}(v_{i,j} + v_{j,i}) \tag{4.2}$$

is the Eulerian strain-rate. Outside the band the velocity field is denoted by v_i^0. Inside the band the deformation is also homogeneous with the possibility of a uniform shearing parallel to t superimposed on v_i^0 according to

$$v_{i,j}^b = \dot{a} t_i \nu_j + v_{i,j}^0. \tag{4.3}$$

The rate of change of ω, defined as before in Fig. 1, is related to $\dot{a}$ by

$$\dot{\omega} = \dot{a} \cos^2(\psi - \omega) - \dot{\epsilon} \sin 2\omega \tag{4.4}$$

where $\dot{\epsilon} = \epsilon_{11}^0$ is still the strain-rate outside the band. Continuity of traction-rate across the band interfaces can be expressed as

$$(\dot{n}_{ij}^b - \dot{n}_{ij}^0)\nu_i \nu_j = 0 \quad \text{and} \quad (\dot{n}_{ij}^b - \dot{n}_{ij}^0)\nu_i t_j = 0 \tag{4.5}$$

where n_{ij} are the components of the unsymmetric nominal stress tensor (the first Piola–Kirchhoff stress) referred to the x_i-axes and $\dot{n}_{ij}$ are the increments, or rates, of these components.

As before, let σ_{ij} and $\overset{*}{\sigma}_{ij}$ be the Cartesian components of the Cauchy stress and its Jaumann-rate and let s_{ij} and $\overset{*}{s}_{ij}$ be their respective deviator components. The 3-dimensional incremental constitutive relation is written as

$$\overset{*}{s}_{ij} = L_{ijkl}\dot{\epsilon}_{kl} \tag{4.6}$$

where $\dot{\epsilon}_{pp} = 0$ and the hydrostatic part, $\dot{\sigma}_{pp} = \overset{*}{\sigma}_{pp}$, is independent of the strain-rate. The instantaneous moduli L in the current state will, in general, have more than one branch depending on $\dot{\epsilon}$; they are taken to be independent of hydrostatic pressure. The components share the indicial symmetries

$$L_{ijkl} = L_{jikl} = L_{ijlk} = L_{klij}. \tag{4.7}$$

Using the connection

$$\dot{n}_{ij} = \overset{*}{s}_{ij} + \frac{1}{3}\dot{\sigma}_{pp}\delta_{ij} + \sigma_{ik}v_{j,k} - (\sigma_{ik}\dot{\epsilon}_{jk} + \sigma_{jk}\dot{\epsilon}_{ik}) \tag{4.8}$$

one can write

$$\dot{n}_{ij} = c_{ijkl}v_{l,k} + \frac{1}{3}\dot{\sigma}_{pp}\delta_{ij} \tag{4.9}$$

where

$$c_{ijkl} = L_{ijkl} + \frac{1}{2}\sigma_{ik}\delta_{lj} - \frac{1}{2}\sigma_{il}\delta_{kj} - \frac{1}{2}\sigma_{jk}\delta_{li} - \frac{1}{2}\sigma_{jl}\delta_{ki}. \tag{4.10}$$

The two equations (4.5) expressing continuity of traction-rate can be used to solve for $\dot{a}$ and $\dot{\sigma}_{pp}^b - \dot{\sigma}_{pp}^0$ in terms of $v_{i,j}^0$ (i.e. in terms of $\dot{\epsilon}$):

$$\dot{a}c_{ijkl}^b \nu_i t_j \nu_k t_l = -(c_{ijkl}^b - c_{ijkl}^0)\nu_i t_j v_{l,k}^0 \tag{4.11}$$

$$\frac{1}{3}(\dot{\sigma}_{pp}^b - \dot{\sigma}_{pp}^0) = -\dot{a}c_{ijkl}^b \nu_i \nu_j \nu_k t_l - (c_{ijkl}^b - c_{ijkl}^0)\nu_i \nu_j v_{l,k}^0. \tag{4.12}$$

The branch of $\mathbf{L}^b$ entering in the above must be consistent with $\dot{\epsilon}^b$ and similarly for $\mathbf{L}^0$. The hydrostatic part of the stress outside the band, σ^0_{pp}, may be specified arbitrarily and (4.12) then gives the rate at which σ^b_{pp} deviates from σ^0_{pp}. One can show explicitly that only the difference $\sigma^b_{pp} - \sigma^0_{pp}$ actually enters into (4.11) and (4.12).

For the perfect block, $\mathbf{c}^b = \mathbf{c}^0$ prior to bifurcation so that $\dot{a} = 0$ and $\dot{\sigma}^b_{pp} - \dot{\sigma}^0_{pp} = 0$ until

$$c_{ijkl}\nu_i t_j \nu_k t_l = 0. \tag{4.13}$$

This is the shear band bifurcation condition as derived by Hill[1] which leads to (2.6) (see Appendix II of [6]).

For an imperfect block and moduli $\mathbf{L}^b$ and $\mathbf{L}^0$ evolve differently once plastic deformation sets in so that $\dot{a}$ and $\dot{\sigma}^b_{pp} - \dot{\sigma}^0_{pp}$ are nonzero from the start of plastic straining. The growth of the band is determined from the incremental equations (4.11) and (4.12).

Shear band growth in a kinematic hardening solid

Prager's kinematic yield surface and hardening rule is adopted. With α_{ij} as a deviator tensor specifying the current center of the yield surface, the yield condition is

$$\frac{3}{2}\tilde{s}_{ij}\tilde{s}_{ij} = \sigma_y^2 \tag{4.14}$$

where $\tilde{s}_{ij} = s_{ij} - \alpha_{ij}$ and σ_y is the initial yield stress which fixes the size of the yield surface. The material is assumed to be incompressible. The tensor of instantaneous moduli defined by (4.6) is

$$L_{ijkl} = \frac{2}{3}EI_{ijkl} - (E - E_t)\tilde{s}_{ij}\tilde{s}_{kl}/\sigma_y^2 \tag{4.15}$$

assuming (4.14) holds and $\tilde{s}_{ij}\dot{\epsilon}_{ij} > 0$, while the second part of (4.15) is excluded otherwise. In (4.15),

$$I_{ijkl} = \frac{1}{2}(\delta_{ik}\delta_{jl} + \delta_{il}\delta_{jk}) - \frac{1}{3}\delta_{ij}\delta_{kl} \tag{4.16}$$

E is Young's modulus and E_t is the tangent modulus of the uniaxial true stress-logarithmic strain curve at the stress level $\sigma_y + (3\alpha_{ij}\alpha_{ij}/2)^{1/2}$. The translation of the yield surface is specified by the finite strain generalization

$$\overset{*}{\alpha}_{ij} = \frac{3}{2}\tilde{s}_{ij}\tilde{s}_{kl}\overset{*}{\sigma}_{kl}/\sigma_y^2 \tag{4.17}$$

for plastic loading and $\overset{*}{\alpha}_{ij} = 0$ otherwise, where $\overset{*}{\alpha}$ is the Jaumann-rate of α.

The uniaxial stress–strain behaviour is represented by a piecewise power-law

$$\sigma/\sigma_y = E\epsilon/\sigma_y \quad \text{for} \quad \epsilon \le \sigma_y/E \quad \text{and} \quad \sigma/\sigma_y = (E\epsilon/\sigma_y)^N \quad \text{for} \quad \epsilon > \sigma_y/E \tag{4.18}$$

With σ_y^b denoting the yield stress in the band and σ_y^0 that outside, the imperfection amplitude is here defined as

$$\bar{\xi} = (\sigma_y^0 - \sigma_y^b)/\sigma_y^0 \tag{4.19}$$

so that $\bar{\xi} > 0$ corresponds to a softer material in the band.

Growth of the shear band is shown in Fig. 5 for an initial orientation $\psi_l = 11.45°$ and for a material with $\sigma_y/E = 0.005$ and $N = 0.2$. In the case $\bar{\xi} = 0.01$ localization takes place at $\epsilon_{max} = 0.81$, at which strain elastic unloading occurs outside the band so that ϵ remains essentially unchanged as ω increases in magnitude. A similar behaviour is found for the smaller inhomogeneity, $\bar{\xi} = 0.001$, at a higher strain $\epsilon_{max} = 1.02$. However, for the negative imper-

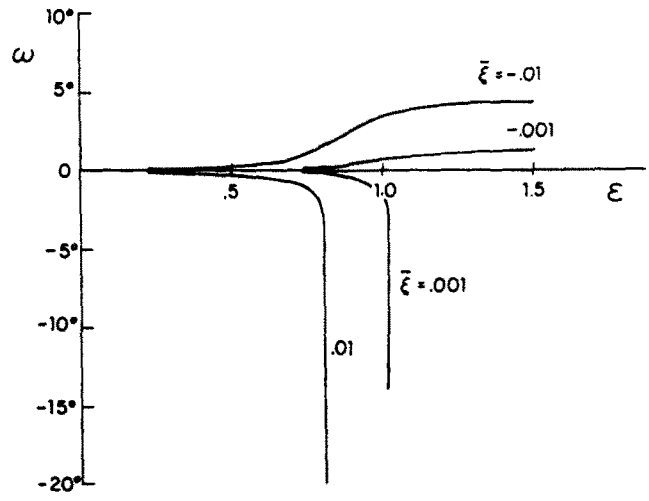

Fig. 5. Growth of a shear band in a kinematically hardening solid with $\sigma_y/E = 0.005$ and $N = 0.2$, for various initial inhomogeneities. The initial band orientation is $\psi_I = 11.45°$.

fections, ω only grows a small amount and no localization occurs, although this response is also artificial.

As the band grows, a discontinuity develops in the stress component acting parallel to the band, i.e. in $\sigma_{tt} \equiv \sigma_{ij}t_it_j$. The jump in σ_{tt} across the band interface as a function of the strain ϵ outside the band is shown in Fig. 6 for the cases of Fig. 5. For the cases in which the band material is softer ($\bar{\xi} > 0$) the jump in σ_{tt} results in a larger effective stress in the band than outside it promoting localization. In part, this explains why shear bands are possible in a hardening material.

The dependence of the localization strain ϵ_{max} on the initial inclination angle ψ_I is shown in Fig. 7 for two imperfection levels, again with $N = 0.2$. Also shown as dashed-line curves is the strain ϵ where the rotation in the band attains the level $\omega = -1°$, and it can be seen that localization occurs at strains just beyond this relatively low level of rotation. For $\bar{\xi} = 0.01$ the lowest value of ϵ_{max} is 0.52 and is associated with $\psi_I = 26°$; for $\bar{\xi} = 0.001$ the corresponding values are $\epsilon_{max} = 1.02$ at $\psi_I = 12°$. If ψ_I is too large, localization does not occur at all since then the band will have rotated past the 45°-range and thus past being critical, at strains which are smaller than the minimum in Fig. 7.

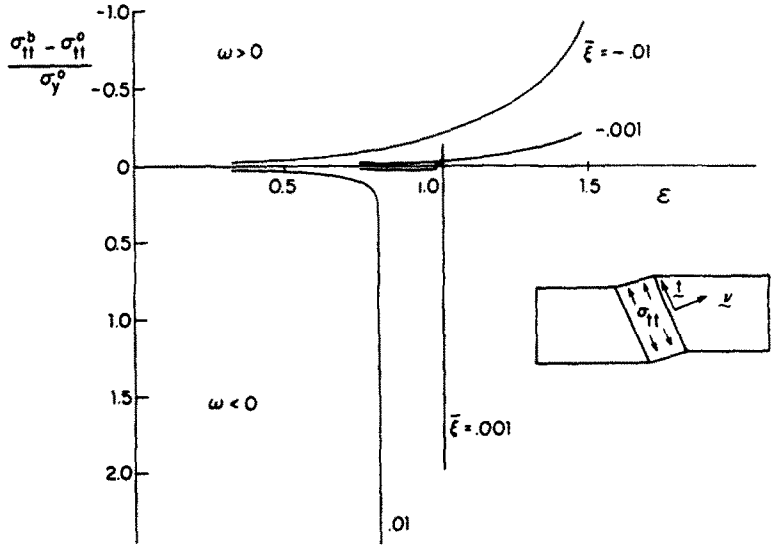

Fig. 6. Jump in $\sigma_{tt} = \sigma_{ij}t_it_j$ across band interface for the kinematically hardening solid with $\sigma_y/E = 0.005$, $N = 0.2$ and $\psi_I = 11.45°$.

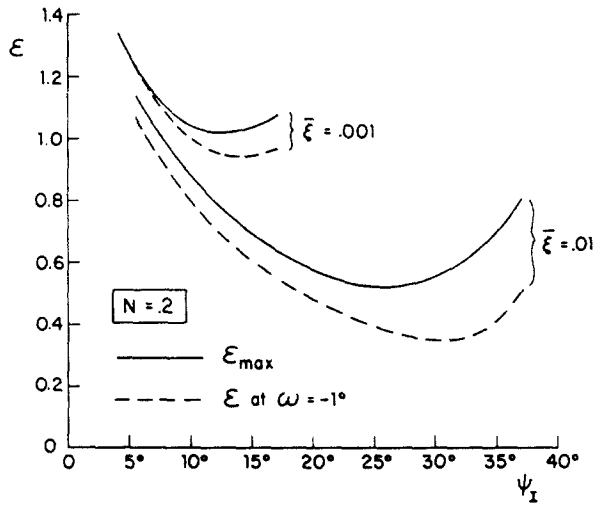

Fig. 7. Localization strain ϵ_{max} vs initial band orientation ψ_I for a kinematically hardening solid with $\sigma_y/E = 0.005$ and $N = 0.2$.

Figure 8 shows curves similar to those in Fig. 7, but for a material with lower strain hardening ($N = 0.1$). For this material the critical localization strain corresponding to $\bar{\xi} = 0.01$ is smaller than that found in Fig. 7, but for the smaller imperfection, $\bar{\xi} = 0.001$, the localization occurs at a larger strain. Also, for this low hardening material the localization strain increases very rapidly as ψ_I exceeds the angle corresponding to the minimum value of ϵ_{max}, and for slightly larger ψ_I no localization is found.

A most interesting aspect of the results of Figs. 7 and 8 is that, for a realistic level of material inhomogeneity, localization into shear bands is predicted by a theory of plasticity with a smooth yield surface which retains the classical assumptions of normality and plastic incompressibility. Kinematic hardening was found to play a similar role in the analysis of localization strains in thin sheet necking in the study by Tvergaard[17]. In the present shear band problems, the yield surface has translated the equivalent of about $2\sigma_y$ for $N = 0.2$ when localization sets in and about $0.7\sigma_y$ for $N = 0.1$. Compared to a surface characterized by isotropic hardening, the curvature of the kinematic hardening surface is substantially greater, which lowers the stress change needed to develop shearing in the band. In this sense, the kinematic surface functions in somewhat the same manner as a corner on a yield surface, which we now investigate.

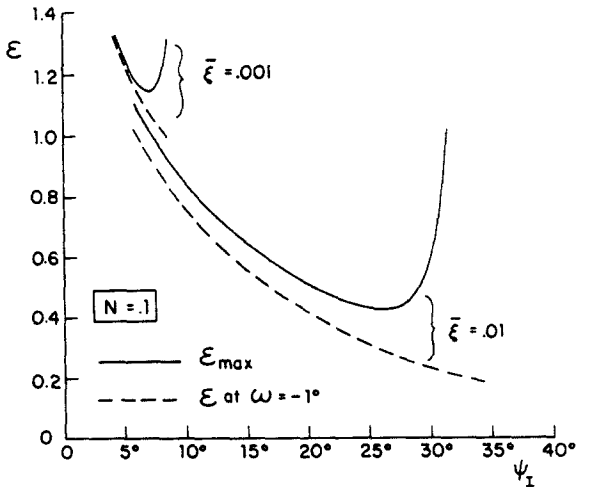

Fig. 8. Localization strain ϵ_{max} vs initial band orientation ψ_I for a kinematically hardening solid with $\sigma_y/E = 0.005$ and $N = 0.1$.

Shear band growth in a solid which develops a corner on its yield surface

A finite strain version of J_2 corner theory[7] will be employed here as a phenomenological representation of a solid which develops a corner on its yield surface. Elasticity will be neglected and thus the corner theory characterizes a generalized rigid-plastic solid. For the most part, the notation used here follows that of [7].

The corner theory is constructed to coincide with a finite strain J_2 deformation theory[17] for a limited range of deformation histories called total loading. The J_2 deformation theory characterizes an incompressible, isotropic non-linearly elastic solid which in the 3-dimensional principal axes of stress and strain satisfies

$$\epsilon_i = \frac{3}{2}\frac{1}{E_s(\sigma_e)} s_i \tag{4.20}$$

where s_i and ϵ_i are the principal stress deviator and logarithmic strain components. With

$$\epsilon_e = (2\epsilon_i\epsilon_i/3)^{1/2} \quad \text{and} \quad \sigma_e = (3s_is_i/2)^{1/2}, \tag{4.21}$$

$E_s(\sigma_e)$ is the secant modulus of the uniaxial true stress-logarithmic strain curve at σ_e and this function must be chosen to fit uniaxial data according to $E_s = \sigma_e/\epsilon_e$. The incremental form of J_2 deformation theory is[18]

$$\overset{*}{s}_{ij} = D_{ijkl}\dot{\epsilon}_{kl} \tag{4.22}$$

where

$$D_{ijkl} = \frac{2}{3}E_sI_{ijkl} - (E_s - E_t)s_{ij}s_{kl}\sigma_e^{-2} + Q_{ijkl} \tag{4.23}$$

and where $E_t = \mathrm{d}\sigma_e/\mathrm{d}\epsilon_e$. In principal axes only the "shearing" components of Q are nonzero with

$$Q_{1212} = Q_{2121} = Q_{1221} = Q_{2112} = \frac{E_s}{3}\left\{\frac{3(s_1 - s_2)}{2E_s}\coth\left[\frac{3(s_1 - s_2)}{2E_s}\right] - 1\right\} \tag{4.24}$$

and with similar expressions for Q_{1313} and Q_{2323}.

With s as the current stress deviator at the loading point on the yield surface, the yield surface in the vicinity of s is a generalized cone whose axis passes through s and the origin of stress space. A positive angular measure β of the direction of the stress-rate from the cone axis is defined by

$$\cos\beta = \sqrt{\left(\frac{3}{2}\right)}\sigma_e^{-1}s_{ij}\overset{*}{s}_{ij}/(\overset{*}{s}_{mn}\overset{*}{s}_{mn})^{1/2} = \mathrm{sign}\,(s_1)\overset{*}{s}_{11}/(\overset{*}{s}{}^2_{11} + \overset{*}{s}{}^2_{12})^{1/2} \tag{4.25}$$

where the second expression is specialized to the plane strain, principal stress axes. The opening of the cone is specified by $0 < \beta < \beta_c$, where β_c is a parameter satisfying $(\pi/2) < \beta_c < \pi$; for $\beta > \beta_c$ the material is rigid. In the calculations reported below, β_c is prescribed to be a fixed value during the deformation history. A sharp corner is modelled by a relatively large value of β_c, while a blunt corner is associated with values of β_c only slightly larger than $\pi/2$.

A positive angular measure ϕ of the direction of the strain-rate from the cone axis is defined as[7]

$$\cos\phi = \sqrt{E_t}\sigma_e^{-1}s_{ij}\dot{\epsilon}_{ij}/(D_{ijkl}\dot{\epsilon}_{ij}\dot{\epsilon}_{kl})^{1/2} = \mathrm{sign}\,(s_1)\dot{\epsilon}_{11}/(\dot{\epsilon}^2_{11} + h^2\dot{\epsilon}^2_{12})^{1/2} \tag{4.26}$$

where the second expression holds in the principal stress axes in plane strain and where

$$h = \left[\frac{3s_1}{E_s}\coth\left(\frac{3s_1}{E_s}\right)\frac{E_s}{E_t}\right]^{1/2}. \tag{4.27}$$

The rate-constitutive relation is specified by the stress-rate functional

$$W = \frac{1}{2}g(\phi)D_{ijkl}\dot{\epsilon}_{ij}\dot{\epsilon}_{kl} \tag{4.28}$$

according to

$$\overset{*}{s}_{ij} = L_{ijkl}(\phi)\dot{\epsilon}_{kl} \tag{4.29}$$

where

$$L_{ijkl}(\phi) = \frac{\partial^2 W}{\partial\dot{\epsilon}_{ij}\partial\dot{\epsilon}_{kl}}. \tag{4.30}$$

The function $g(\phi)$, which provides the transition from total loading to unloading, is taken to be specified by[7]

$$\left.\begin{aligned} g &= 1 && 0 \le \phi \le \theta_0 \\ &= (1-x^3)^{-2} && \theta_0 < \phi < \theta_n \end{aligned}\right\} \tag{4.31}$$

where $x = (\phi - \theta_0)/(\theta_n - \theta_0)$, and where θ_0 and θ_n are parameters defined below. A total loading increment is one for which $\phi \le \theta_0$ such that the behaviour coincides with J_2 deformation theory (i.e. $\mathbf{L} = \mathbf{D}$). For $\theta_0 < \phi < \theta_n$, $g(\phi)$ provides a smooth transition, consistent with convexity requirements, to rigid incremental response for $\phi \to \theta_n$. Thus, θ_n specifies the forward cone of normals, within which the strain-rate falls. In the case of plane strain with elastic strains neglected, which is being considered here, one can show that θ_n is related to the cone angle β_c by

$$\theta_n = \arctan\left[(\tan\beta_c)/h\right] - \frac{\pi}{2}. \tag{4.32}$$

In the calculations reported below, the angle θ_0 specifying the total loading regime is taken as a fixed fraction of θ_n.

This completes the specification of the version of J_2 corner theory used here. An explicit formula for $\mathbf{L}$ in terms of $g(\phi)$ and $\mathbf{D}$ is obtained along lines similar to the development in Section 2(iv) of [7]. Calculations were performed for a material with a true stress-logarithmic strain curve given by

$$\sigma_e = K\epsilon_e^N \tag{4.33}$$

which reduces to (3.3) in plane strain where $k = (2/\sqrt{3})^{N+1}K$.

Since the corner theory coincides with the power-law elastic material for total loading responses, the perfect block of corner theory material under plane strain tension will bifurcate at precisely the same strain as the elastic material in (3.6) and Fig. 2, if bifurcation takes place in such a way that total loading does indeed occur within the band. If the elastic material itself bifurcates in such a way that $\phi < \theta_0$, then the post-bifurcation behaviours of the two materials will coincide until ϕ exceeds θ_0. For the choice of parameters in the examples presented below, the elastic material does not bifurcate in a manner such that $\phi < \theta_0$. Thus the constraint $\phi \le \theta_0$ must be *imposed* on the bifurcation solution (4.3) in the band and this permits the determination

of $\dot{a}$ and $d\omega/d\epsilon$ immediately following bifurcation. If

$$\tan 2\psi > -h \operatorname{cotan} \theta_0, \tag{4.34}$$

one can show that bifurcation takes place with $\phi = \theta_0$ in the band and $\phi = 0$ ($d\epsilon > 0$) outside. The initial slopes of the two branches of the bifurcation solutions are

$$\frac{d\omega}{d\epsilon} = \frac{2\cos^2\psi}{\cos 2\psi(\tan 2\psi \pm h \operatorname{cotan} \theta_0)} \tag{4.35}$$

corresponding to $d\omega < 0$ for the plus and $d\omega > 0$ for the minus. However, if

$$\tan 2\psi < -h \operatorname{cotan} \theta_0, \tag{4.36}$$

there is just one bifurcation solution with $\phi = \theta_0$ in the band and $\phi = 0$ outside. It is given by (4.35) with the minus sign corresponding to $d\omega > 0$ with $d\epsilon > 0$. The other solution has $\phi < \theta_0$ in the band and a rigid response ($d\epsilon = 0$ with $\dot{\sigma} < 0$) outside such that $d\omega < 0$. Illustrations of each of these possibilities will be seen in the figures below.

Four numerical examples based on J_2 corner theory with $N = 0.1$ are presented in Figs. 9–12. In the first three examples in Figs. 9–11, the initial orientation of the band is chosen as $\psi_I = 35.8°$ corresponding to the critical orientation $\psi_c = 54.2°$ with $\epsilon_c = 0.32$ for the perfect block, as in the examples in Fig. 2 for the nonlinear elastic material. The initial slopes of the bifurcation solutions are shown as short dashed-line segments emanating from ϵ_c, and these slopes are determined from (4.35) since (4.34) holds in all three examples. In Fig. 12, $\psi_I = 15°$ corresponding to a bifurcation strain in the perfect block of $\epsilon = 0.68$. In this instance (4.36) holds.

The yield surface corner in the example of Fig. 9 is rather sharp with $\beta_c = 135°$. The total loading range is taken as $\theta_0 = \theta_n/2$, so that coupled with a sharp corner is a large total loading range. It can be seen that a very small imperfection in the form of a softer band material, $\bar{\xi} > 0$, where

$$\bar{\xi} = (K_0 - K_b)/K_0, \tag{4.37}$$

leads to localization at a strain ϵ_{max} below ϵ_c. For the case $\bar{\xi} = 0.001$, for example, the shear band develops to $\omega \cong -1°$ whereupon the material outside the band unloads and becomes rigid. From that point on, all deformation is confined to the band. The response for the negative-signed imperfection, $\bar{\xi} = -0.001$, is included for completeness.

To draw contrast with the above results for the sharp corner, Fig. 10 shows what happens when the yield surface has a relatively blunt corner with $\beta_c = 115°$. Here again the total loading

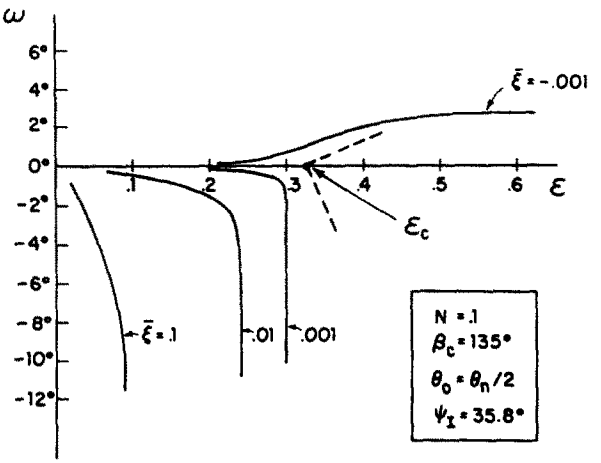

Fig. 9. Growth of a shear band in a solid that develops a rather sharp corner on the yield surface, for various initial inhomogeneities. Dashed lines show initial post-bifurcation slopes for a homogeneous solid.

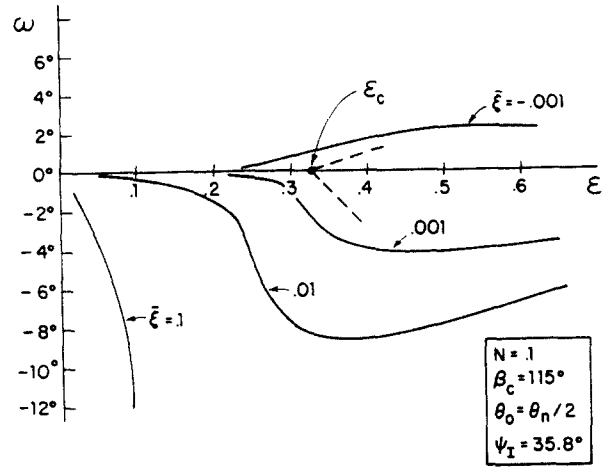

Fig. 10. Growth of a shear band in a solid that develops a relatively blunt corner on the yield surface, for various initial inhomogeneities. Dashed lines show initial post-bifurcation slopes for a homogeneous solid.

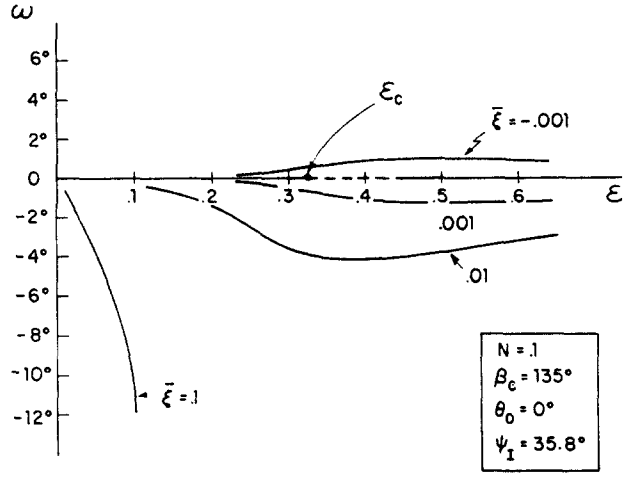

Fig. 11. Growth of a shear band in a solid that develops a sharp yield surface corner, but no total loading range. The initial post-bifurcation slopes are zero, as indicated by dashed line.

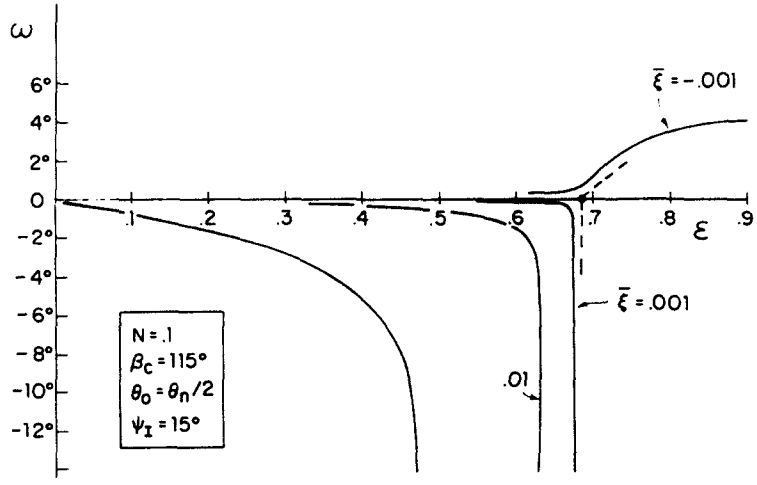

Fig. 12. Growth of a shear band in a slice of material that reaches the critical orientation considerably after the smallest critical strain. The yield surface corner is relatively blunt.

range is taken to occupy one half of the forward cone of normals ($\theta_0 = \theta_n/2$). Now the stiffening effect, which occurs as soon as total loading ceases and which is emphasized by the blunt corner, does not allow the localization process to "run away", except at the very large imperfection $\bar{\xi} = 0.1$. Instead, deformation outside the band continues and localization in the band saturates. This effect is seen even more dramatically in Fig. 11 where the cone angle is sharp ($\beta_c = 135°$) but the total loading range has been set to zero ($\theta_0 = 0°$). With $\theta_0 = 0°$, stiffening sets in for any increment which departs from proportional loading (i.e. from $\phi = 0$) and the shear band only experiences relatively mild shearing, except when the imperfection is large. (Bifurcation in the perfect block still occurs at $\epsilon_c = 0.32$ when $\theta_0 = 0$ but, from (4.35), it does so with $d\omega/d\epsilon = 0$ on both solution branches.)

Figure 12 should be contrasted with Fig. 10, since all parameters are the same ($\beta_c = 115°$, $\theta_0 = \theta_n/2$, $N = 0.1$) except that the initial orientation ψ_I is 15° in Fig. 12 which is well below the initial orientation $\psi_I = 35.8°$ associated with critical bifurcation in Fig. 10. Consequently, the bifurcation strain ($\epsilon = 0.68$) is more than twice that in Fig. 10 and, even in the presence of imperfections, shear band formation is correspondingly postponed. When the band does start to develop, however, it quickly succumbs to run-away localization in Fig. 12, while it does not in Fig. 10. The responses in Fig. 12 are not unlike those for the kinematic hardening material in Fig. 5. The stiffening effect of the blunt corner is not sufficient to hold back localization at the higher stress level acting on the band when it has rotated into the critical orientation range. By contrast, in Fig. 10 the stiffening effect at the lower stresses is able to retard the growth of the shear band to the point where the band has rotated past the range of criticality.

Plots of the strain outside the band at localization, ϵ_{max}, are shown as a function of initial band orientation in Fig. 13 for two sets of corner parameters for $\bar{\xi} = 0.01$. Also shown is the strain level at which ω has grown to $-2°$. The main difference between the two cases is that the minimum value of ϵ_{max} is larger than the critical bifurcation strain ($\epsilon_c = 0.32$) for the solid with a blunt corner on its yield surface, whereas it is slightly less for the solid with the sharp corner.

Some of the features described above appear to be in qualitative accord with the observations made by Anand and Spitzig[8] in their experimental study of shear band formation in a high strength maraging steel under plane strain tension and compression. By deforming block specimens to various levels of strain, by slicing the specimens and by etching, these workers were able to ascertain the strain at which the first shear bands set in. Their material has low, but positive, strain hardening and the bands set in at a relatively small strain which was actually lower than the prediction based on deformation theory. No porosity was observed. The orientations of the bands satisfied $\psi > 45°$ in tension and $\psi < 45°$ in compression, in accord with the theory. One can infer that localization did saturate in most of the bands, since at overall strains well beyond the point where the bands first were observed the material still maintained its integrity, but the number of bands had multiplied significantly. At a sufficiently high strain at least one band did experience run-away localization and the material failed.

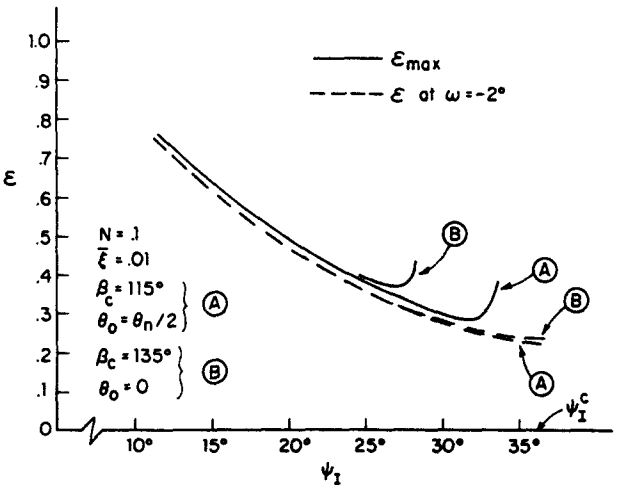

Fig. 13. Localization strain as a function of initial band orientation for two sets of corner theory parameters. In all cases $\bar{\xi} = 0.01$ and $N = 0.1$.

Acknowledgements—The work of John W. Hutchinson was supported in part by grants from the National Science Foundation, DMR-77-24295 and ENG-78-10756, and by The Division of Applied Sciences, Harvard University.

REFERENCES

1. R. Hill, Acceleration waves in solids. *J. Mech. Phys. Solids* **10**, 1–16 (1962).
2. J. W. Rudnicki and J. R. Rice, Conditions for the localization of deformation in pressure-sensitive dilatant materials. *J. Mech. Phys. Solids* **23**, 371–394 (1975).
3. J. R. Rice, The localization of plastic deformation. *Proc. 14th Int. Congr. Theor. Appl. Mech.* (Edited by W. T. Koiter), pp. 207–220. North-Holland, Amsterdam (1976).
4. H. Yamamoto, Conditions for shear localization in the ductile fracture of void-containing materials. *Int. J. Fracture* **14**, 347–365 (1978).
5. A. Needleman and J. R. Rice, Limits to ductility set by plastic flow localization. *Mechanics of Sheet Metal Forming* (Edited by D. P. Koistinen and N-M. Wang), pp. 237–267. Plenum Press, New York (1978).
6. R. Hill and J. W. Hutchinson, Bifurcation phenomena in the plane tension test. *J. Mech. Phys. Solids* **23**, 239–264 (1975).
7. J. Christoffersen and J. W. Hutchinson, A class of phenomenological corner theories of plasticity. *J. Mech. Phys. Solids* **27**, 465–487 (1979).
8. L. Anand and W. A. Spitzig, Initiation of localized shear bands in plane strain. *J. Mech. Phys. Solids* **28**, 113–128 (1980).
9. V. Tvergaard, A. Needleman and K. K. Lo, Flow localization in the plane strain tensile test. Materials Research Laboratory, NRL E-123, Brown University (March 1980).
10. J. K. Knowles and E. Sternberg, Discontinuous deformation gradients near the tip of a crack in finite anti-plane shear: an example. *J. Elasticity* **10**, 81–110 (1980).
11. R. Abeyaratne, Discontinuous deformation gradients away from the tip of a crack in anti-plane shear. Materials Research Laboratory, MRL E-122, Brown University (Jan. 1980).
12. S. Nemat-Nasser, A. Shokooh and M. Taya, On localized deformations in biaxial tension. *Tech. Rep. N* 79-2-13, Department of Civil Engineering, Northwestern University, (Feb. 1979).
13. R. Hill, Constitutive inequalities for isotropic elastic solids under finite strain. *Proc. Roy. Soc. London* **A314**, 457–472 (1970).
14. J. K. Knowles and E. Sternberg, On the failure of ellipticity and the emergence of discontinuous deformation gradients in plane finite elastostatics. *J. Elasticity* **8**, 329–379 (1978).
15. W. T. Koiter, Over de stabiliteit van het elastisch evenwicht. Thesis, Delft, H. J. Paris, Amsterdam (1945). English transl.: NASA TT F-10, 833 (1967); and AFFDL-TR-70-25 (1970).
16. B. Budiansky, Theory of buckling and post-buckling behavior of elastic structures. *Advances in Applied Mechanics* (Edited by C. S. Yih), Vol. 14, p. 2. Academic Press, New York (1974).
17. V. Tvergaard, Effect of kinematic hardening on localized necking in biaxially stretched sheets. *Int. J. Mech. Sci.* **20**, 651–658 (1978).
18. J. W. Hutchinson and K. W. Neale, Sheet necking—II. Time-independent behavior. *Mechanics of Sheet Metal Forming* (Edited by D. P. Koistinen and N-M. Wang), pp. 127–153. Plenum Press, New York (1978).